NATIONAL ADVISORY COMMITTEE FOR AERONAUTICS

TECHNICAL NOTE 3801

EXPERIMENTAL INVESTIGATION OF THE STRENGTH OF MULTIWEB BEAMS WITH CORRUGATED WEBS

By Allister F. Fraser

Langley Aeronautical Laboratory
Langley Field, Va.

Washington

October 1956

W

NATIONAL ADVISORY COMMITTEE FOR AERONAUTICS

TECHNICAL NOTE 3801

EXPERIMENTAL INVESTIGATION OF THE STRENGTH OF MULTIWEB BEAMS WITH CORRUGATED WEBS

By Allister F. Fraser

SUMMARY

The results of an experimental investigation of the strength of multiweb beams with corrugated webs are reported. Included in the investigation were two types of connection between the web and the skin. A comparison between the structural efficiency of corrugated-web and channel-web multiweb beams is presented, and it is shown that, for a considerable range of the structural index, corrugated-web beams can be built which are structurally more efficient than channel-web beams.

INTRODUCTION

Attention has been directed to the use of corrugated webs in thin-wing construction as a means of reducing stresses associated with nonuniform temperature distribution in a structure. Compared with more conventional webs, a corrugated web can offer only a slight restraint to thermal expansion of wing skins.

Upon closer examination of the properties of corrugated sheet as a web, it appears that other advantages over more conventional webs can be realized. Corrugated webs, because of their high moment of inertia, are capable of supplying very stiff deflectional and rotational restraints to a skin if an adequate connection is made. In addition, information exists which indicates that corrugated sheet is very efficient in carrying shear loads (refs. 1 and 2).

The purpose of the investigation herein described was to evaluate experimentally the ultimate bending strength of corrugated-web beams at room temperature and to acquire an indication of their structural efficiency.

SYMBOLS

A_i	area per chordwise inch (see p. 5)
A_i/h	solidity parameter
B	total width of beam, in.
b	web spacing, in.
h	total beam depth including skins, in.
l	length of beam, in.
M_i	moment per chordwise inch
M_i/h^2	structural index, ksi
t_s	thickness of skin, in.
δ	beam shortening, in.
σ_A	stress in connection angles at beam failure, ksi
σ_{cr}	stress in compression skin at buckling, ksi
σ_s	stress in compression skin at beam failure, ksi

TEST PROGRAM AND SPECIMENS

Nine three-cell multiweb beams with corrugated webs were fabricated for this investigation. The beams were divided into two groups which differed principally in the type of the connection between the corrugated webs and the skins.

The first group (beams 1 to 4, table I) had web-skin connections which provided only a negligible restraint to thermal expansion of the skin. The connections were made with an individual clip angle between the web and the skin at each corrugation crest. (See fig. 1(a).) In the second group (beams 5 to 9, table I) some of the desirable thermal characteristics were sacrificed in an attempt to improve the load-carrying ability of this type of beam. The individual clip angles were

replaced by continuous angles (see fig. 1(b)) which will offer a small restraint to expansion of the skin if the beams are subjected to a non-uniform temperature distribution.

In order to show the equivalence of bending and compression tests for determining the value of failing stress in the compression skin, beams 1 and 3 were loaded with a pure bending moment and beams 2 and 4 were axially loaded flat-end columns. This equivalence was anticipated because the rotational and deflectional restraint of the skin provided by a corrugated web is essentially independent of the bending or compression loads acting on the web. The beams of the second group, those with continuous angle connections, were tested to failure as short flat-end columns in compression.

Pertinent dimensions of the beams are given in table I. The skins of all beams were 1/8-inch-thick 7075-T6 aluminum-alloy sheet. All webs were clad 2024-T3 aluminum-alloy corrugated sheet 0.032 inch thick. (See fig. 2.) In beams 1 to 4 the clip angles were extruded 2024-T4 aluminum-alloy angles 1/16 by 3/4 by 3/4 inch and were 1 inch long. A single 1/4-inch rivet (AN442AD-8-8) connected each clip angle to the corrugated web and two 3/16-inch rivets (AN442AD-6-8) held each clip angle to the skin. The center line of the rivets connecting the clip angles to the skin was 7/16 of an inch from the corrugation crest.

Beams 5 to 9 were nominally identical with each other except for the web spacing and the length of the beams. The web spacing was varied to give nominal ratios of web spacing to skin thickness of 25, 30, 40, 50, and 60, and the length of each beam was adjusted so that it was approximately five times the web spacing. The web-skin connections were extruded 7075-T6 aluminum-alloy continuous angles 3/32 by 3/4 by 1 inch. In order to facilitate the riveting of the angles to the webs, one angle from each pair at a web connection was scalloped as shown in figure 1(b), and the hatched area shown in figure 3 was considered to carry the load in the stress analysis of the beams. This scalloping also reduces the area capable of resisting thermal expansion of the skin. In both the angle-skin and the angle-web connections 3/16-inch rivets (AN442AD-6-7) were used. The rivet pitch in the angle-skin connections was 0.89 inch and the center line of the rivets was 3/8 inch from the corrugation crest.

TEST PROCEDURE AND INSTRUMENTATION

The skins of the beams tested in bending were bolted to end fixtures, and the beams were loaded to failure under a pure bending moment in the combined load testing machine of the Langley structures research laboratory. The ends of the compression beams were ground flat, square, and parallel, and the beams were compressed to failure in a universal testing machine.

Strains in the skins of the beams at various locations were measured with the use of Baldwin SR-4 type strain gages and were recorded automatically against applied load by an automatic strain recorder. The resulting load-strain plots were used to obtain the load at which skin buckling occurred. For the compression tests, continuous load-shortening plots were also recorded. To measure the shortening, the impulse to the recorder was supplied by strain gages mounted at the root of a flexible cantilever beam whose tip deflection was the same as the shortening of the test beam. The load-shortening curves were used to substantiate the value of critical load obtained from the load-strain plots as well as to obtain information from which the load carried by the various elements of the beams at failure could be computed.

RESULTS

Typical failures of beams with clip angle connections and with continuous angle connections are shown in figure 4. Failure in both types of beams occurred when the out-of-plane forces associated with buckling distortions of the skin were sufficient to pull rivets out of the corrugated webs. It was evident from the skin failing stress (table II) that the relatively flexible clip angle connections were not as effective as continuous angle connections in utilizing the high deflectional and rotational restraint offered by a corrugated web for stabilization of the skin.

The maximum loads for the beams are given in table II. Also shown are values of the stress in the skin and in the connection angles at beam failure. The calculation of the stresses in beams 1 to 4 was made under the assumption that the bending moments and compression loads were resisted by the skins only.

The calculation of the stresses in beams 5 to 9 was based on the assumption that the connection angles remained unbuckled until failure. Furthermore, only the area of the scalloped angles shown hatched in figure 3 was assumed to carry load. The latter assumption is supported by the fact that the slope of the elastic parts of the curves of average stress against unit shortening, as shown in figure 5, is in agreement with Young's modulus. The stress in the connection angles at beam failure was obtained by taking the unit shortening at failure from figure 5 and reading the stress corresponding to that strain from the stress-strain curve shown in figure 6. The load carried by the connection angles was then subtracted from the failing load on the specimen to obtain the load carried by the skins.

The results for beams 1 to 4 verify the assumption, mentioned previously, that corrugated-web beams will fail at the same skin stress in

bending as in compression (table II). This result was used as justification for testing the remaining five beams in compression.

The buckling and failing stresses of beams 5 to 9 are plotted in figure 7. Also shown are results for beams with channel webs that were obtained from reference 3. The web spacing b used in computing values of the ratio b/t_s is the distance between web center lines for both the corrugated-web beams and the channel-web beams. The web spacing, defined in this manner, does not represent an unsupported width of skin in the case of the corrugated-web beams, and buckling stresses in excess of the theoretical values for clamped-edge plates unsupported in the width b (buckling coefficient of 6.98) were usually encountered. The buckling stresses shown for channel webs are based on the assumption of simple support at the webs (buckling coefficient of 4.00). The failing stresses for the corrugated-web beams are correspondingly high compared with the result shown for channel-web beams.

The high failure stresses for the load-carrying elements of corrugated-web beams do not necessarily lead to a high strength-weight efficiency for the beam as a whole under a bending moment because of the weight of non-load-carrying elements in the construction. This is exemplified in figure 8, where the efficiency of the corrugated-web test beams is compared with that of optimum channel-web beams (from ref. 3) with the same nominal value of h/t_s. In this figure the solidity A_i/h, which is a measure of weight, is plotted against the structural index M_i/h^2 for a beam in bending. The parameter A_i is defined as the area per chordwise inch of compression material and its supporting structure for a beam with many bays. For the test beams, this area includes the area of the corrugated web, the compression connection angles, and the compression skin. The conversion of compression data to bending strength was accomplished by multiplying the failing loads in the connection angles and skin by the respective distances of their centroids from the centroids of the opposite angles and skin and totaling the results.

A comparison of beams 1 to 4 with beams 5 to 9, as plotted in figure 8, illustrates the superiority of continuous angle connections over clip angle connections for this type of beam. The corrugated-web beams with continuous angle connections also show an improvement in efficiency over channel-web beams for a large part of the range of structural index and are at least as efficient as the channel-web beams over the entire test range.

ANALYSIS AND DISCUSSION

An extension of the test results shown in figures 7 and 8 is presented in figure 9. In addition, the optimum-weight envelope for

channel-web beams, as determined in reference 3, is shown along with a hypothetical maximum-efficiency curve for multiweb construction. The latter curve corresponds to achievement of a skin stress equal to the material yield stress without supporting webs. The extension of the present data is based on the assumption that the failing stresses in the connection angles and in the skin are independent of beam depth for a reasonable range of beam depths. The assumption is valid only if web crushing does not occur and if the rotational stiffness of the web is not appreciably diminished as the beam depth is increased. Web crushing will not occur until the Euler load for the web is reached, and it is not a problem with corrugated webs in the range of depths considered. The rotational stiffness of the web is dependent primarily on the design of the connection to the skin, which is not a function of beam depth, and on the moment of inertia of the corrugated web in the vicinity of the connection. The bending moments transmitted from the buckled plate to the web are of a sinusoidal nature and, as such, are self-equilibrating. They can, therefore, be expected to "wash out" in a distance of approximately a buckle length, which is less than the beam depth for the beams considered.

The calculated curves presented in figure 9 indicate that the weight of a corrugated-web beam of optimum design for a given value of the structural index may be considerably less than that for channel-web beams of optimum design. An envelope curve of minimum-weight designs has not been drawn inasmuch as relatively few of the many possible design variables in the corrugated-web type of construction were considered in the present investigation. It is believed, however, that a minimum-weight envelope established by an extensive test program would not be appreciably lower than that indicated by the curves presented in figure 9.

The test results have not been extended to shallower beams than those actually tested because the test data are not realistic for beams having a large stress variation throughout the depth of the connection angles. This depthwise stress variation also tends to make the large connection angles required in this construction inefficient as load-carrying members.

Figure 9 was constructed from test data which are restricted to one combination of web, connection angle, and skin thickness. Extension of these results to other combinations will not be valid unless substantiated by tests. For example, the use of smaller ratios of web thickness to skin thickness or the use of weaker web-skin connections may result in premature failure. A premature failure of this type was reported in reference 4, where a wing with corrugated webs was tested in bending.

CONCLUDING REMARKS

The results of an investigation of the strength of multiweb beams with corrugated webs and with two types of connections are reported. It is established that the connection between web and skin greatly affects the maximum strength and structural efficiency of corrugated-web beams. The results of this investigation have been analyzed and applied to beams of greater depth. This analysis shows that corrugated-web beams can be built with better structural efficiency than channel-web beams over a wide range of structural index.

Langley Aeronautical Laboratory,
National Advisory Committee for Aeronautics,
Langley Field, Va., June 14, 1956.

REFERENCES

1. Seydel, Edgar: Schubknickversuche mit Wellblechtafeln. Jahrb. 1931 der DVL E. V. (Berlin-Aldershof), pp. 233-245.

2. Shanley, F. R.: Weight-Strength Analysis of Aircraft Structures. McGraw-Hill Book Co., Inc., 1952, p. 39.

3. Rosen, B. Walter: Analysis of the Ultimate Strength and Optimum Proportions of Multiweb Wing Structures. NACA TN 3633, 1956.

4. The Bristol Aeroplane Company Limited: The Application of "Redux" Adhesive to Aircraft Structures. S & T Memo No. 5/54, British Ministry of Supply, TPA 3/TIB, Apr. 1954.

TABLE I.- BEAM DIMENSIONS

Beam	Web-skin connection	Loading	b, in.	t_s, in.	B, in.	b/t_s	l, in.	h, in.
1	Clip angle	Bending	4.74	0.1223	17.01	38.7	34.18	5.27
2	Clip angle	Compression	4.75	.1220	17.01	38.9	33.87	5.25
3	Clip angle	Bending	7.21	.1239	24.50	58.2	46.08	5.30
4	Clip angle	Compression	7.25	.1216	24.52	59.6	45.76	5.27
5	Continuous angle	Compression	3.13	.1193	11.62	26.2	17.33	5.25
6	Continuous angle	Compression	3.705	.1208	13.52	30.7	19.87	5.24
7	Continuous angle	Compression	5.02	.1202	17.26	41.7	25.48	5.24
8	Continuous angle	Compression	6.25	.1200	21.02	52.1	33.32	5.24
9	Continuous angle	Compression	7.50	.1201	24.74	62.3	38.73	5.24

TABLE II.- TEST RESULTS

Beam	Loading	σ_S, ksi	σ_A, ksi	Maximum load
1	Bending	36.2	----	389.0 in-kips
2	Compression	35.3	----	148.6 kips
3	Bending	24.0	----	370.0 in-kips
4	Compression	25.0	----	149.5 kips
5	Compression	67.3	71.5	340.0 kips
6	Compression	64.4	67.5	341.0 kips
7	Compression	47.0	62.6	324.0 kips
8	Compression	38.8	65.0	329.0 kips
9	Compression	33.0	67.0	335.0 kips

(a) With clip angle connections. L-92724.1

Figure 1.- Corrugated-web multiweb beams.

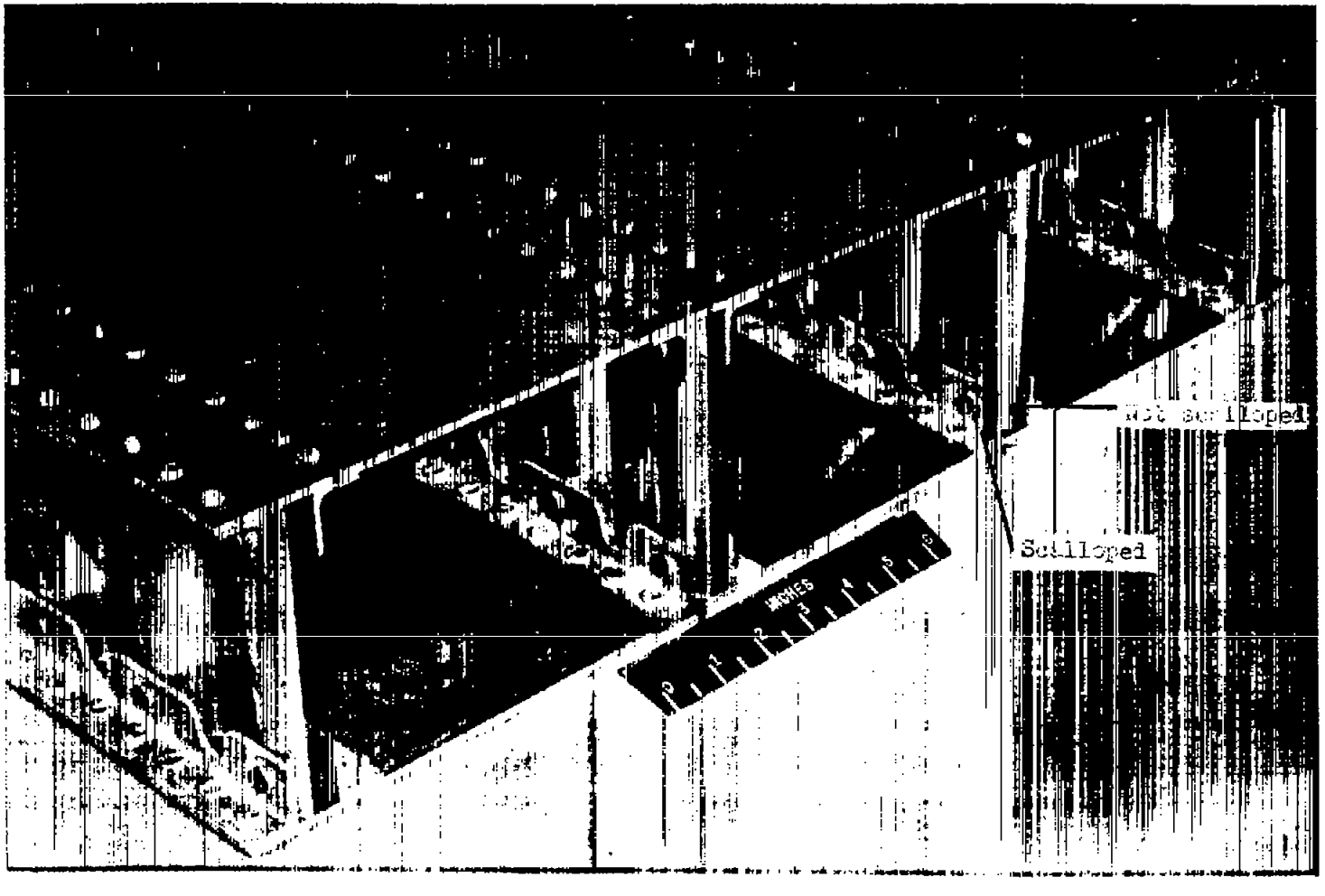

(b) With continuous angle connections. L-92723.1

Figure 1.- Concluded.

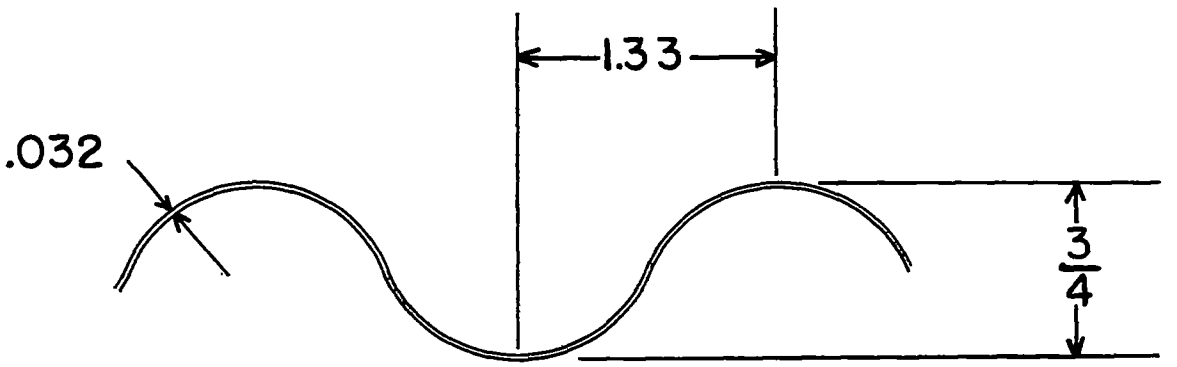

Figure 2.- Circular-arc corrugated sheet of 2024-T3 clad aluminum alloy.

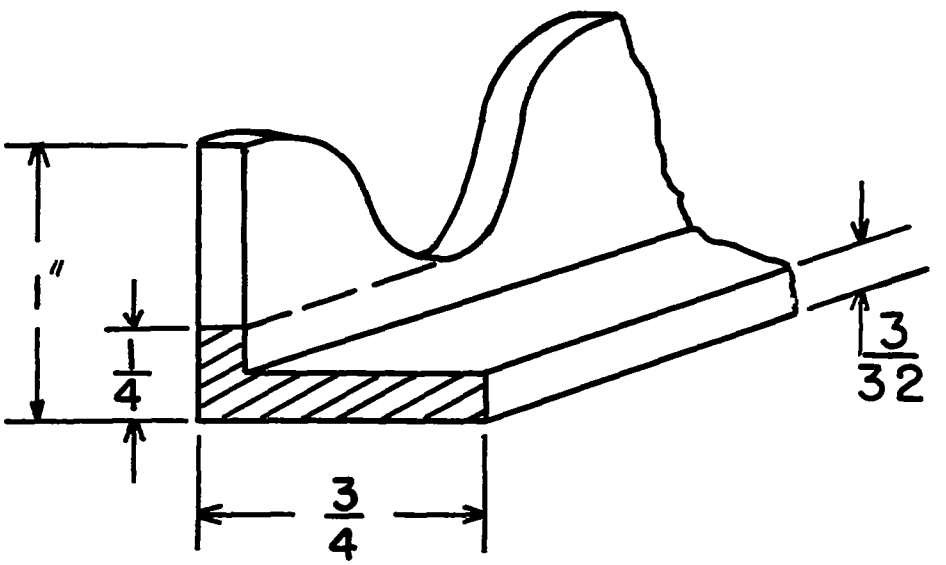

Figure 3.- Scalloped connection angle with load-carrying area hatched.

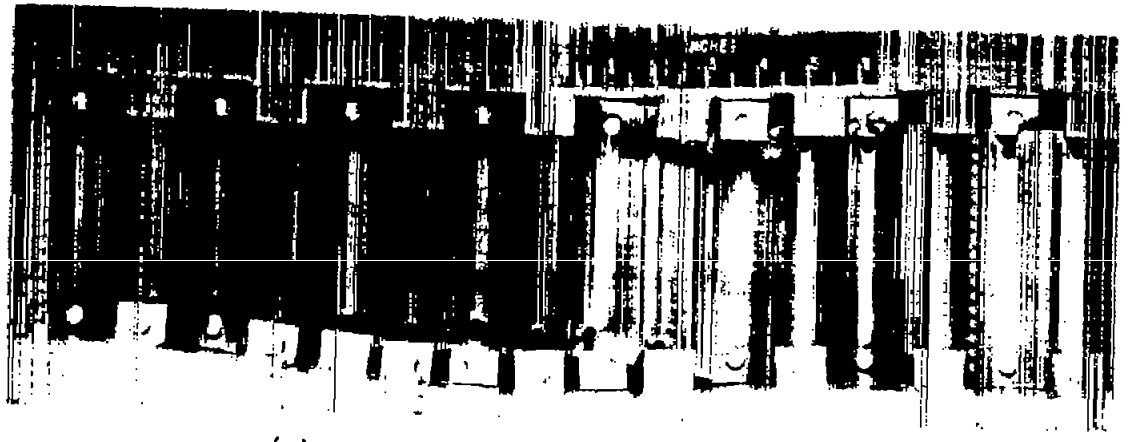

(a) With clip angle connections. L-93291

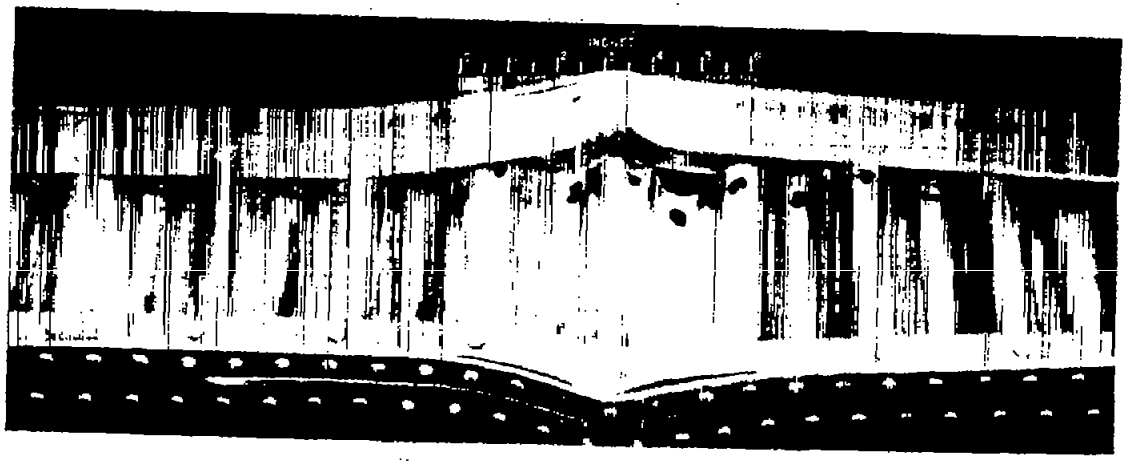

(b) With continuous angle connections. L-93292

Figure 4.- Typical failures.

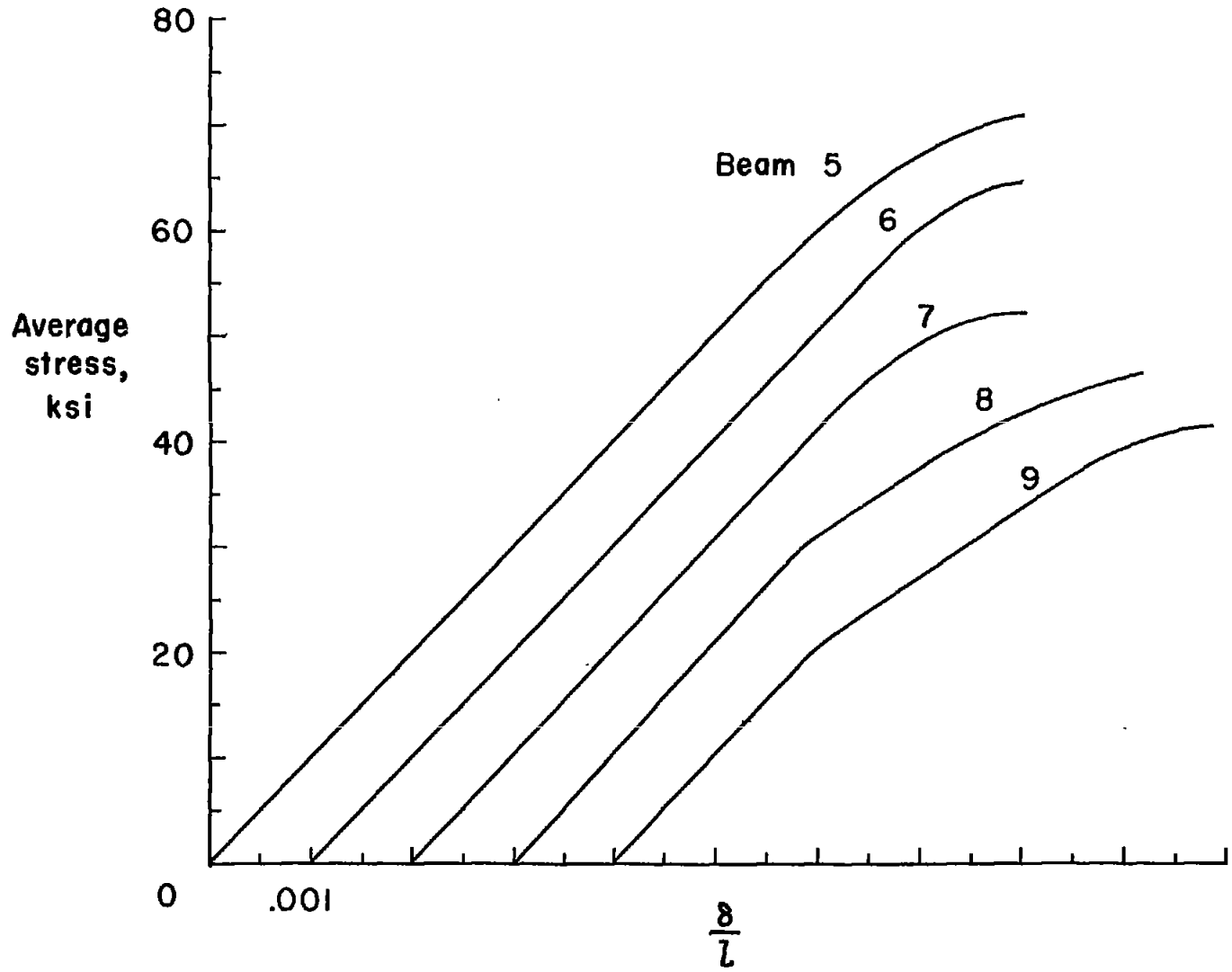

Figure 5.- Average stress plotted against unit shortening for beams 5 to 9.

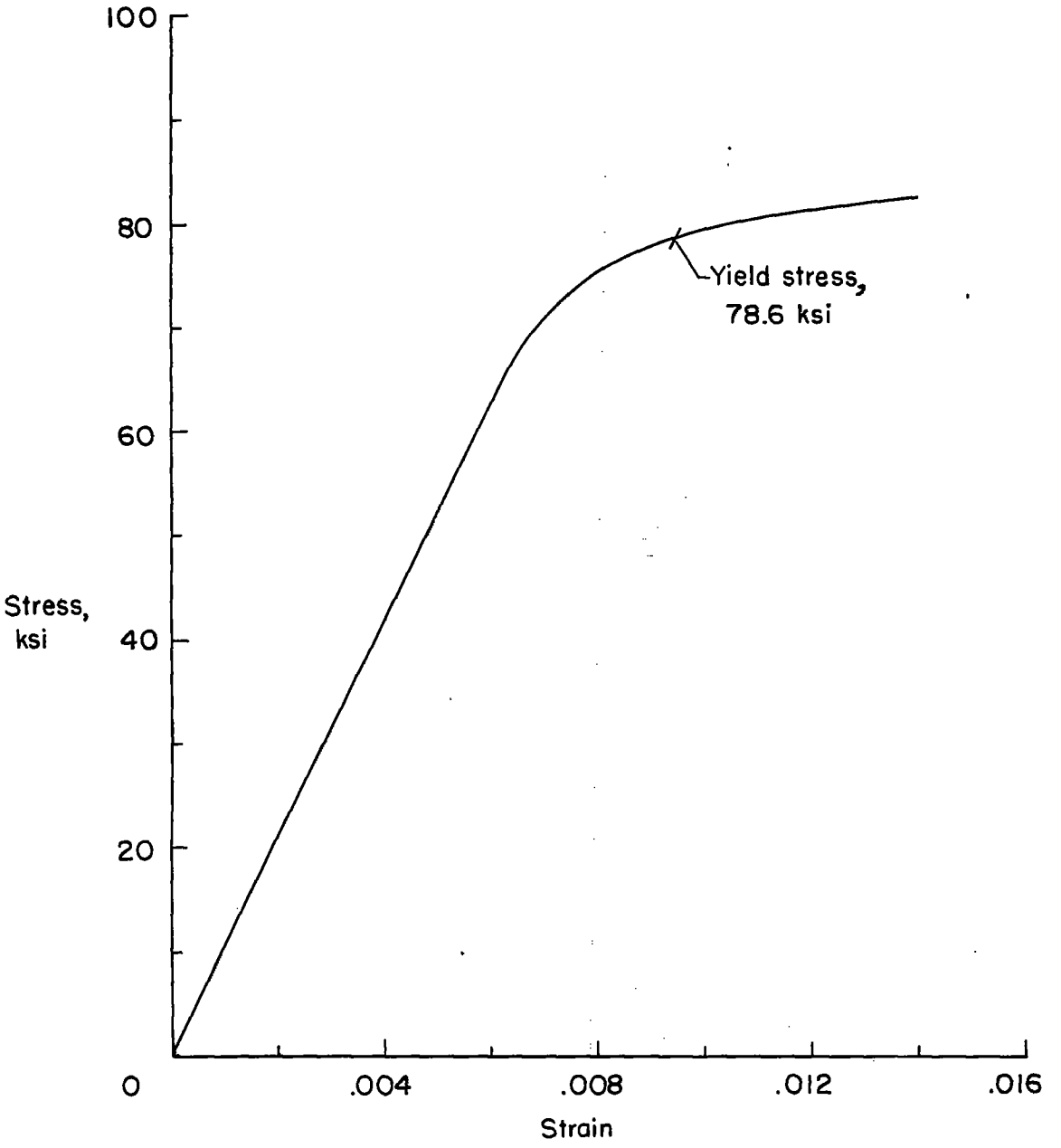

Figure 6.- Typical compression stress-strain curve for extruded 7075-T6 aluminum alloy.

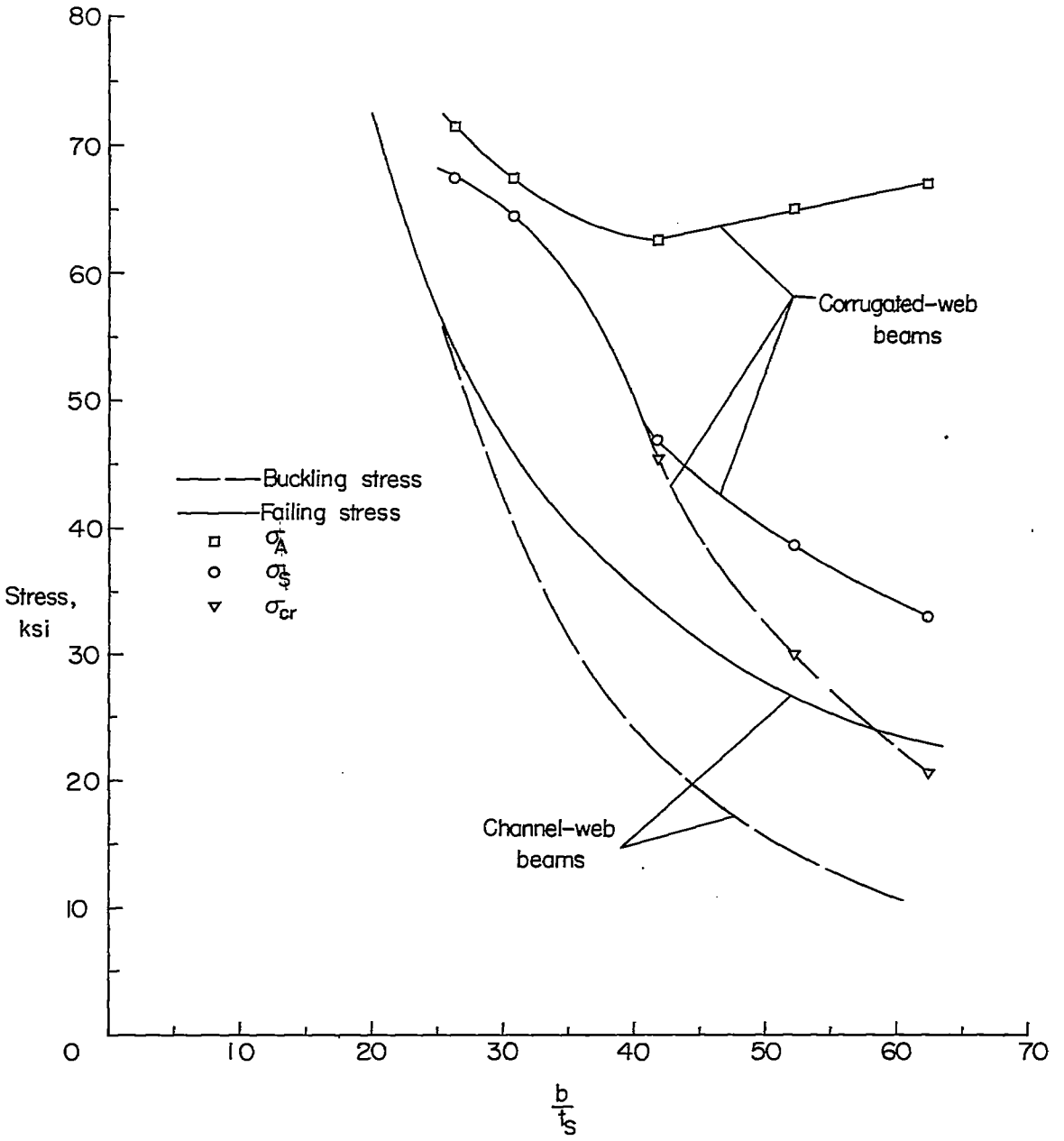

Figure 7.- Buckling and failing stresses in components of corrugated-web beams 5 to 9 and in channel-web beams.

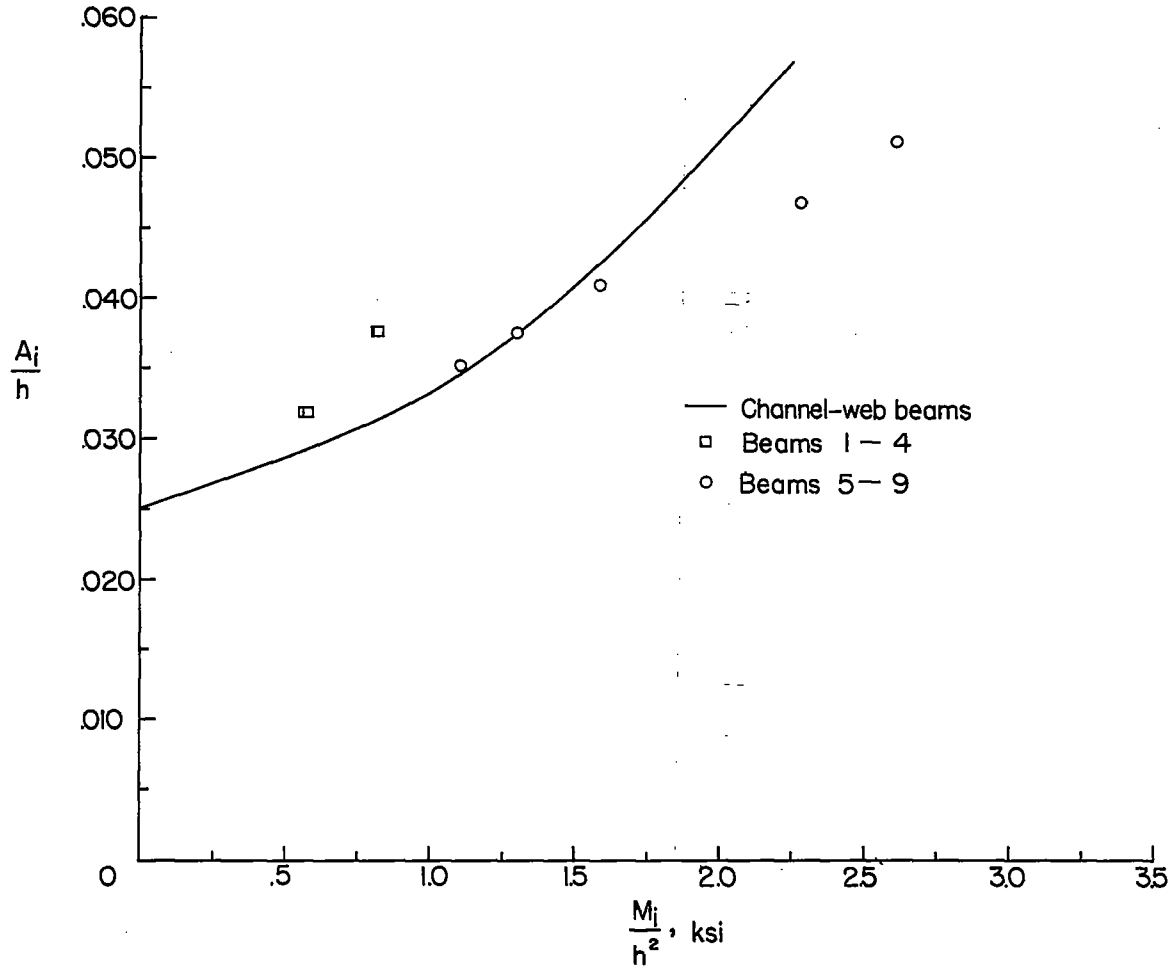

Figure 8.- Structural efficiency of corrugated-web beams and optimum channel-web beams. $h/t_g \approx 40$.

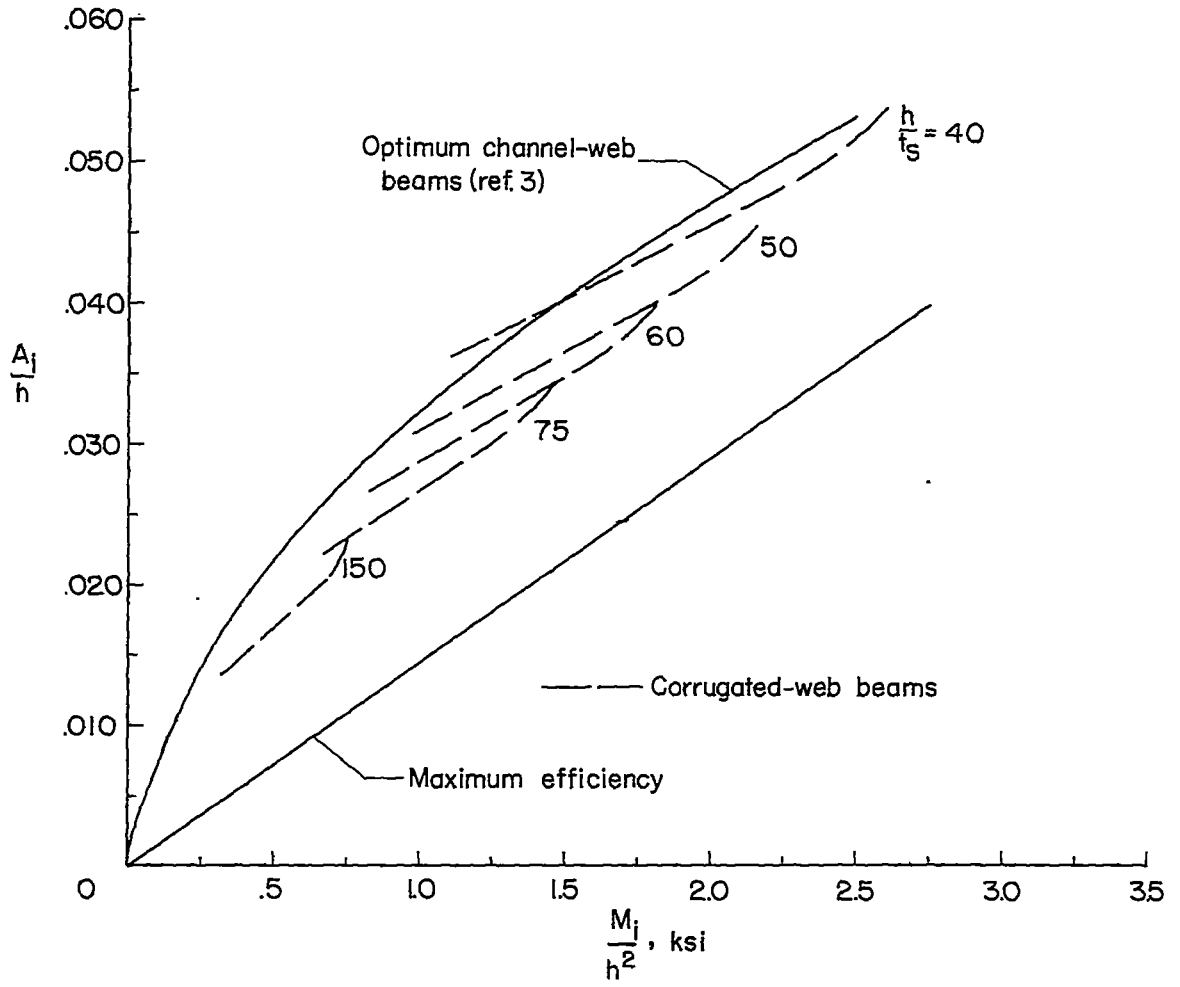

Figure 9.- Optimum envelope for channel-web beams (ref. 3) and extension of results for corrugated-web beams 5 to 9.